

VELOCITY AND ORIENTATION CONTROL IN AN ELECTRICAL WHEELCHAIR ON AN INCLINED AND SLIPPERY SURFACE

S. O. Onyango¹, Y. Hamam² and K. Djouani³

¹*F'SATI-Tshwane University of Technology, Pretoria, South Africa*

²*ESIEE-Paris, Paris Est University, Noisy-le-Grand, France*

F'SATI - Tshwane University of Technology, Pretoria, South Africa

LISV laboratory, UVSQ Velizy, Versailles, France

³*LISSI Laboratory, Paris Est University, Val de Marne, France*

F'SATI - Tshwane University of Technology, Pretoria, South Africa

Keywords: Modelling, Gravity, Input-output linearization, Slip, Control, Wheelchair.

Abstract: People with disability increase everyday due to accidents, poor health care and aging of the population. While some of these disabled people are strong enough and can comfortably use manual wheelchairs to move, others are too weak and may find it extremely difficult to drive powered wheelchairs with basic functionalities. Wheelchairs adaptable to various specialized functionalities may therefore be important if mobility of the severely disabled persons is to be ensured. Control parameters adaptable to hand, tongue or even head joysticks may consequently be necessary. Authors of this paper considered linear velocity and angular position for control. With such control parameters the wheelchair user may navigate and reach every desired location. To mimic real outdoor situations, slippery, inclined and flat surfaces are also considered. The dynamic modelling procedure used in this paper is based on the Euler-Lagrange formalism. The wheelchair platform considered in this paper is a differential drive platform with two passive front caster wheels and two active rear wheels.

1 INTRODUCTION

Thousands of people with disability worldwide take advantage of wheelchair for their daily (Vignier et al., 2008; Woude et al., 2006; Wobbrock et al., 2004). A number of these disabled persons drive their wheelchairs out-of-doors. In such environments, they encounter extremely bumpy and slippery road surfaces making it very difficult for the wheelchair to navigate. Such adverse road conditions may consequence into dangerous slipping of the wheelchair platform and result into severe accidents to the already disabled wheelchair user. Dynamic modelling process should as a result consider adverse ground characteristics and the topographies of the road upon which the wheelchair will be moving. The majority researchers base their work on the kinematic models of wheelchair platforms in modelling, (Tarokh and McDermott, 2005; Zhu et al., 2006). Such models however fail to account for the acceleration and can significantly differ from the actual movement whenever the handling limits of the wheelchair are approached. Dynamic modelling as a result becomes

the only option if accurate analysis of wheelchair is to be ensured. Most of the researchers have considered dynamic modelling in their research (Dixon et al., 2001; Kozlowski and Pazderski, 2004; Motte and Guy, 2000; Stonier et al., 2007; Williams et al., 2002), however such work restrict the platforms to flat surfaces alone and for that reason do not account for the variations on gravitational forces affecting wheelchair during its motion on inclined surfaces. Other researchers have also taken into account frictional forces in dynamic modelling (Williams et al., 2002; Sidek, 2008; Kozlowski and Pazderski, 2004; Hamed et al., 2007). In this work a dynamic model of wheelchair platform is considered. This model accounts for gravitational forces, frictional forces and slipping effects.

Control of nonlinear systems is among the very challenging fields of research. This is because there lacks a generic method for controller synthesis (Isidori, 1995; Khalil, 1996). Few of the possible methods consist of feedback linearization and Lyapunov functions (Isidori, 1995). For the latter, there is no systematic way of construction of the func-

tion except for passive systems (Spong et al., 1989), the former is the other method considered in this paper. Input–output feedback linearization linearizes only part of the dynamics between the output and input. Feedback linearization has been used earlier in (Ortega et al., 2000). With this method, nonlinearities are pushed to the internal dynamics in order that the behavior of input–output is minimum phase. Nonlinear state transformation and nonlinear state feedback is then used to recompense system nonlinearities. A linear controller is then designed and employed to control the linearized system (Ortega et al., 2000). This paper is organized as follows. In section II the dynamic model of an electric powered wheelchair which includes dynamics of friction and gravity forces of uphill and downhill movements is presented. Input–output feedback linearization is utilized in section III to control linear velocity and angular position. Finally in section IV, detailed simulation results are presented to lay bare the importance of the proposed modelling and control techniques. Some concluding remarks are also presented.

2 DYNAMIC MODEL OF THE WHEELCHAIR

2.1 A Nonholonomic Wheelchair

In this work, we consider the structure of wheelchair platform shown in fig.1 for modeling and control. Fig. 1 consists of two independently driven motorized hind and two passive front castor wheels. Based on the differential drive principle, authors of this paper consider angular velocity of the wheelchair platform above as a function of the difference between angular velocities of right and left wheels. It is possible to achieve a straight line trajectory whenever equal torques are

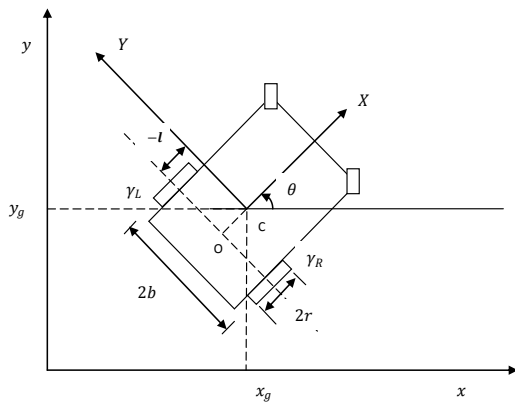


Figure 1: Platform of the differential drive wheelchair.

applied to each of the rear wheels with identical motors. The wheelchair platform herein is considered as a rigid body in derivation of the kinetic energy. Lagrange formalism is then used to derive the general set of differential equations that describes the time evolution of wheelchair subject to nonintergrable kinematic constraints (Hamed et al., 2007; Wells, 1967).

In fig.1, components of the coordinate vector are shown. The inertial coordinate frame is indicated as (x, y, z) while the body fixed coordinate of the wheelchair is indicated as (X, Y, Z) with c being the origin. The position of the wheelchair in the inertial frame is specified completely by; $q = [x_g, y_g, z_g, \theta]^T$, where, x_g , y_g and z_g are the coordinates of the of the wheelchair platform's centre of gravity, the orientation of the wheelchair is described by θ while the road inclination angle is indicated as ϕ according to fig.2. $2b$ is the length of the axis between the wheels of the wheelchair platform and r is the radius of the wheels. γ_R and γ_L are the angular rotations of the right wheel and the left wheel respectively. The Lagrange function \mathcal{L} which is difference between kinetic and potential energies of the wheelchair may be expressed as (Hamed et al., 2007; Wells, 1967);

$$\begin{aligned} \mathcal{L} = & \frac{1}{2}M(\dot{x}_g^2 + \dot{y}_g^2 + \dot{z}_g^2) + \\ & \frac{1}{2}I_z\dot{\theta}^2 + Ml\dot{\theta}\cos\phi(\dot{x}_g\sin\theta - \dot{y}_g\cos\theta) \\ & - Mg\sin\phi(x_g\cos\theta + y_g\sin\theta) \end{aligned} \quad (1)$$

where;

$$M = M_w + M_p$$

M_p is the patients mass, M_w is the total mass of wheelchair plus its components, I_z is the moment of inertia of the wheelchair platform about z_g , g is the gravitational acceleration. With n as the dimensional configuration space and $q = (q_1, \dots, q_n)$ as the generalized coordinates subjected to $(n - m)$ constraints, the general expression of a nonholonomic wheelchair may be illustrated by (Wells, 1967; Fierro and Lewis, 1997);

$$M(q)\ddot{q} + C(q, \dot{q})\dot{q} + F + G(q) = E(q)\tau + A^T(q)\lambda \quad (2)$$

where;

$M(q) \in \mathbb{R}^{n \times n}$ is the symmetric positive definite inertia matrix, $G(q) \in \mathbb{R}^n$ is a vector of gravitational

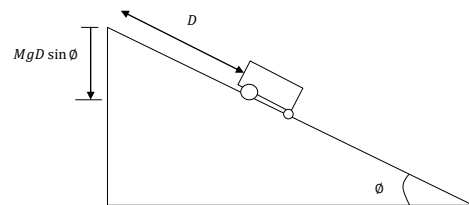


Figure 2: The wheelchair on an incline (D is the displacement on xy -plane).

forces, $C(q, \dot{q}) \in \mathbb{R}^{n \times n}$ is the matrix of corolis and centripetal and forces, $\tau \in \mathbb{R}^r$ is the input vector of torques and forces, F is the matrix of frictional forces, $E(q) \in \mathbb{R}^{n \times r}$ is the input transformation matrix $A(q) \in \mathbb{R}^{(n-m) \times n}$ is the matrix related to non-holonomic constraints and λ is the vector of Lagrange multipliers.

$$M(q) = \begin{bmatrix} M & 0 & 0 & Ml \cos \phi \sin \theta \\ 0 & M & 0 & -Ml \cos \phi \cos \theta \\ 0 & 0 & M & 0 \\ Ml \cos \phi \sin \theta & -Ml \cos \phi \cos \theta & 0 & I_z \end{bmatrix}$$

$$C(q, \dot{q}) = \begin{bmatrix} 0 & 0 & 0 & Ml \dot{\theta} \cos \phi \cos \theta \\ 0 & 0 & 0 & Ml \dot{\theta} \cos \phi \sin \theta \\ 0 & 0 & 0 & 0 \\ 0 & 0 & 0 & 0 \end{bmatrix}$$

$$G(q) = \begin{bmatrix} Mg \sin \phi \cos \theta \\ Ml \sin \phi \sin \theta \\ 0 \\ Mg \sin \phi (y_g \cos \theta - x_g \sin \theta) \end{bmatrix}$$

$$A(q) = \begin{bmatrix} -\cos \phi \sin \theta & \cos \phi \cos \theta & \sin \phi & -d \\ \sin \phi \sin \theta & -\sin \phi \cos \theta & \cos \phi & 0 \end{bmatrix}$$

$$E(q) = \begin{bmatrix} \frac{\cos \theta}{r} & \frac{\cos \theta}{r} \\ \frac{\sin \theta}{r} & \frac{\sin \theta}{r} \\ 0 & 0 \\ \frac{b}{r} & \frac{-b}{r} \end{bmatrix}$$

$$\tau = \begin{bmatrix} \tau_R \\ \tau_L \end{bmatrix}$$

The following are some of the properties of dynamic system (2).

Property 1.

Matrices $M(q)$ and $G(q)$ are bounded and uniformly continuous if q is uniformly bounded and continuous respectively. Matrix $C(q, \dot{q})$ is uniformly bounded and uniformly continuous if \dot{q} is uniformly bounded and continuous (Ge and Lewis, 2006).

Property 2.

Matrice $\dot{M} - 2C$ is skew symmetric, that is, $x^T (\dot{M} - 2C)x = 0 \quad \forall x \neq 0$ (Ge and Lewis, 2006).

We assume first that the platform wheels are subjected to nonholonomic kinematic constraints and therefore the wheels of the platform roll without slipping. These independent and non integrable kinematic constraints confine lateral movements to directions perpendicular to the axis of the driving wheels of the wheelchair and may be expressed in the following form:

$$A(q)\dot{q} = 0 \quad (3)$$

Where $S(q) \in \mathbb{R}^{n \times m}$ is a set of linearly independent and smooth vector field that spans the null space of $A(q)$, it is possible to state that:

$$S^T(q)A^T(q) = 0 \quad (4)$$

where

$$S(q) = \begin{bmatrix} \cos \theta & -l \cos \phi \sin \theta \\ \sin \theta & l \cos \phi \cos \theta \\ 0 & l \sin \phi \\ 0 & 1 \end{bmatrix}$$

On account of (3) and (4), a kinetic model (5) of the wheelchair platform which converts velocities η in the body fixed coordinates to velocities \dot{q} in the inertial coordinates may be demonstrated.

$$\dot{q} = S(q)\eta \quad (5)$$

where $\eta = [\vartheta \ \omega]^T$ where ϑ is the linear velocity and ω is the angular velocity of the centre of gravity of the wheelchair.

Slipping parameters may now be introduced in the general coordinate. Since we assume that slip only occurs in the rear wheels, slipping parameters may as a result be introduced and the kinematic model becomes;

$$\dot{q} = S(q)\eta + \varepsilon \quad (6)$$

where;

$\varepsilon = [\dot{x}_g \ \dot{y}_g \ 0 \ \dot{\theta}_g \ 0 \ 0]^T$ is the slipping component with, \dot{x}_g being the velocity of longitudinal slip, \dot{y}_g is the velocity of lateral slip and $\dot{\theta}_g$ is the rate of deviation due to slip.

2.2 Frictional Force

Usually friction modelling is very complex since it is high nonlinear and because of the fact that it depends on many variables. A simplified approximation is therefore presented and used in the description of friction as a combination of viscous and coulomb friction. It may be expressed as

$$f(\varepsilon) = \mu_{vsc}\varepsilon + \mu_{cmb}Mg \operatorname{sgn}(\varepsilon) \quad (7)$$

with μ_{vsc} and μ_{cmb} being the coefficients of viscous and coulomb friction respectively. Based on the fact that velocity of the wheelchair is relatively low, it may be confirmed that coulomb friction is much greater than viscous friction $\mu_{vsc}\varepsilon$, which may now be neglected to simplify the friction model. As a result of $\operatorname{sgn}(\varepsilon)$, equation (7) is not linear when the slipping velocity ε is zero. It is therefore not differentiable whenever $\varepsilon = 0$. But because a continuous and time differentiable friction model of wheelchair is required, the approximation below is proposed:

$$\operatorname{sgn}(\varepsilon) \approx \frac{2}{\pi} \arctan(k \varepsilon) \quad (8)$$

since its true that $\lim_{k \rightarrow \infty} \frac{2}{\pi} \arctan(k \varepsilon) = \text{sgn}(\varepsilon)$ where ($k \gg 1$) is the constant that determine approximation accuracy. From the expression above, force of friction acting at the wheelchairs centre of mass may be expressed in the matrix below

$$F = \frac{2}{\pi} Mg \cos \phi \begin{bmatrix} \mu_{Xmax} \arctan(k \dot{x}_g) \\ \mu_{Ymax} \arctan(k \dot{y}_g) \\ 0 \\ \mu_{\theta max} \arctan(k \dot{\theta}) \end{bmatrix}$$

2.3 A Slipping Wheelchair

Longitudinal slip is the slip ratio s_r and is calculated as the difference between the actual platform's velocity v and the wheel circumferential velocity $r\dot{\gamma}$. However to limit slip between -1 to 1 , the result is divided by either v or $r\dot{\gamma}$ whichever is greater as shown is (9)

$$s_r = \frac{(r\dot{\gamma} - v)}{r\dot{\gamma}} \quad \text{driving : } (r\dot{\gamma} > v)$$

$$s_r = \frac{(r\dot{\gamma} - v)}{v} \quad \text{braking : } (r\dot{\gamma} < v) \quad (9)$$

We assume in this work as in (Hamed et al., 2007) that velocity of the front wheels will reflect the real velocity of the wheelchair and that due to force effect only rear wheels will slip. Slip is for that reason considered in this work to be the difference between the front wheel velocity v and the rear wheel velocity $r\dot{\gamma}$. Velocity and orientation of the castor wheel can geometrically be calculated as in (Hamed et al., 2007) whenever the wheelchair is reduced into a bicycle model.

2.4 Controllable Dynamic Model

The system in equation (2) is then transformed into the form more appropriate for control. Equation (6) is differentiated with respect to time and the result is substituted into (2) to obtain the following relationship:

$$MS\dot{\eta} + M\dot{S}\eta + M\dot{\varepsilon} + CS\eta + C\varepsilon + F + G = E\tau + A^T\lambda \quad (10)$$

To eliminate the constraint matrix $A^T\lambda$, we multiplying equation (10) by S^T , this gives;

$$S^T MS\dot{\eta} + S^T M\dot{S}\eta + S^T M\dot{\varepsilon} + S^T CS\eta + S^T C\varepsilon + S^T (F + G) = S^T E\tau \quad (11)$$

The dynamic model of wheelchair with slip described in (11) is now capable of moving on roads of various inclinations and may be simplified to form (12).

$$\dot{\eta} = [M_n]\eta + [G_n] + [B]\tau \quad (12)$$

where

$$[M_n] = -(S^T MS)^{-1} (S^T M\dot{S} + S^T CS)\eta$$

$$[G_n] = -(S^T MS)^{-1} (S^T M\dot{\varepsilon} + S^T M\dot{\varepsilon} + S^T C\varepsilon + S^T (F + G))$$

$$[B] = (S^T MS)^{-1} (S^T E)$$

3 DESIGN OF A CONTROLLER

Since the dynamic model of the wheelchair platform in equation (12) is nonlinear, the general mathematical expression for such MIMO systems is

$$\dot{x} = f(x(t), u(t))$$

$$y = h(x(t)) \quad (13)$$

where $x \in \mathbb{R}^n$ is the vector of state variables, $u \in \mathbb{R}^m$ is the vector control input and $y \in \mathbb{R}^m$ is the output vector for the system.

Definition 1. Given $x_0 \in \mathbb{X}$, then \mathbb{X} is an n -dimension differentiable manifold if \exists a neighbourhood \mathbb{V} of x_0 and integer vector (r_1, r_2, \dots, r_m) such that (Slotine and Li, 1991; Feng and Fei, 1998);

1. $L_{g_j} L_f^{r_j} h_i(x) = 0 \quad \forall x \in \mathbb{V}, 1 \leq j \leq m, 1 \leq i \leq m, 0 \leq k \leq r_i - 2$
- 2.

$$\beta(x) = \begin{bmatrix} L_{g_1} L_f^{r_1-1} h_1(x) & \cdots & L_{g_m} L_f^{r_m-1} h_1(x) \\ \vdots & \ddots & \vdots \\ L_{g_1} L_f^{r_1-1} h_m(x) & \cdots & L_{g_m} L_f^{r_m-1} h_m(x) \end{bmatrix}$$

is nonsingular $\forall x \in \mathbb{V}$, we say that (13) has a vector relative degree (r_1, r_2, \dots, r_m) at point x_0 .

Lemma. The necessary and sufficient condition for exact feedback linearization at x_0 for system (13) is that \exists a neighbourhood \mathbb{V} of x_0 and a smooth real valued functions $h_i x \in \mathbb{V}, i = 1, 2, \dots, m$. such that system (13) has a vector relative degree (r_1, r_2, \dots, r_m) at the point x_0 , and $\sum_{i=1}^m r_i = 1$ (Feng and Fei, 1998).

Systems (12) is static state input-output linearizable by regular static state feedback and coordinate transformation if an invertible feedback law of the form (14) exist with v being an auxiliary input and an invertible $\beta(x)$,

$$u = \alpha(x) + \beta(x)v \quad (14)$$

and a coordinate change (15)

$$z = \phi(x) \quad (15)$$

so that the new coordinate has linear and controllable closed loop system. In this work, the output equation (16) is chosen in such a way that it is possible to spell out the task that the wheelchair is required to perform in the most realistic way to enable us built a simple controller without lowering the quality of desired performance. Two control objectives are established; 1). is tracking the desired output linear velocity ϑ and 2) is tracking the desired angular position θ of the wheelchair. The following output vector may now be specified.

$$y(x) = \begin{bmatrix} \vartheta \\ \theta \end{bmatrix} \quad (16)$$

In solving the tracking control problem, the linear velocity error and orientation error is defined as in equation (17) so as to force the tracking error $e = [e_1^1 \ e_1^2]^T$ to zero.

$$e = \begin{bmatrix} \vartheta - \vartheta_r \\ \theta - \theta_r \end{bmatrix} = \begin{bmatrix} e_1^1 \\ e_1^2 \end{bmatrix} \quad (17)$$

A constant reference linear velocity ϑ_r and a reference orientation θ_r which is a function of time is assumed in this problem. As a result, we can now track both constant orientation and orientations which are functions of time

3.1 Relative Degree

The control input u does not appear in the second output component after the first differentiation of equation (17) with respect to time, the decoupling matrix obtained is also singular. This implies that the result may not be partial input-output linearizable. θ is therefore delayed to appear in the second derivative of the output to enable the control input u appear.

$$\begin{bmatrix} \dot{e}_1^1 \\ \dot{e}_1^2 \\ \dot{e}_2^2 \end{bmatrix} = \begin{bmatrix} \dot{\vartheta} - \dot{\vartheta}_r \\ \dot{\theta} - \dot{\theta}_r \\ \dot{\omega} - \dot{\omega}_r \end{bmatrix} \quad (18)$$

$$\begin{bmatrix} \dot{e}_1^1 \\ \dot{e}_1^2 \\ \dot{e}_2^2 \end{bmatrix} = \begin{bmatrix} -g \sin \phi - c - m \\ e_2^2 \\ b - d - n \end{bmatrix} + \begin{bmatrix} \frac{1}{Mr}(\tau_R + \tau_L) \\ 0 \\ \frac{-b}{ar}(\tau_R - \tau_L) \end{bmatrix} \quad (19)$$

where

$$\begin{aligned} a &= Ml^2 \cos 2\phi - I_z \\ b &= \frac{Mg \sin \phi}{a} (y_g \cos \theta - x_g \sin \theta) \\ c &= \ddot{x}_g \cos \theta + \ddot{y}_g \sin \theta \\ d &= \frac{\ddot{\theta}}{2a} (2I_z + d^2 M - d^2 M \cos 2\phi) \end{aligned}$$

$$m = \frac{2g \cos \phi}{\pi} \{ \mu_X \cos \theta \arctan(k \dot{x}_g) + \mu_Y \sin \theta \arctan(k \dot{y}_g) \}$$

$$n = \frac{2Mg \cos \phi}{a\pi} \{ -\mu_X l \sin \theta \cos \phi \arctan(k \dot{x}_g) + \mu_Y l \cos \theta \cos \phi \arctan(k \dot{y}_g) + \mu_\theta \arctan(k \dot{\theta}) \}$$

e^1 has a relative degree of one and e^2 has a relative degree of two, the sum of the component of vector relative degree of (18) is therefore 3. Which is greater than the state dimension 2 of the system. State extension is therefore performed to ensure that sum of the component of vector relative degree is less than or equal to the dimension of the system.

3.2 Control Law

State feedback law that compensates the nonlinearity in the input-output behavior may now be applied. A decoupling matrix with a rank of two and therefore invertible and nonsingular unless $a = 0$ is obtained. The dimensions I_z, M and l should for that reason be chosen in such a way that equation (22) is always invertible.

$$\begin{pmatrix} u_1 \\ u_2 \end{pmatrix} = \begin{bmatrix} L_g e_1^1 \\ L_g L_f e_1^2 \end{bmatrix}^{-1} \left[\begin{pmatrix} v_1 \\ v_2 \end{pmatrix} - \begin{pmatrix} L_f e_1^1 \\ L_f e_1^2 \end{pmatrix} \right] \quad (20)$$

where u is the control variable,

$$\begin{pmatrix} L_f e_1^1 \\ L_f e_1^2 \end{pmatrix} = \begin{bmatrix} -g \sin \phi - c - m \\ b - d - n \end{bmatrix}, \quad (21)$$

$$\begin{pmatrix} L_g e_1^1 \\ L_g L_f e_1^2 \end{pmatrix} = \begin{bmatrix} \frac{1}{Mr} & \frac{1}{Mr} \\ \frac{-b}{ar} & \frac{b}{ar} \end{bmatrix} \quad (22)$$

and

$$\begin{bmatrix} v_1 \\ v_2 \end{bmatrix} = \begin{bmatrix} -K_1 e_1^1 \\ -K_{21} e_1^2 - K_{22} e_2^2 \end{bmatrix} \quad (23)$$

$K_{2's}$ are then chosen in such away that polynomial equation (24) below

$$s^2 + K_{22}s + K_{21} = 0 \quad (24)$$

is Hurwitz.

4 SIMULATION AND RESULTS

Computer simulations are presented in this section to confirm the behavior of the designed dynamic model and controller. The wheelchair is simulated on an inclined wet surface and inclined oily surface. Table

Table 1: The dynamic model.

Kinematics	$b = 0.35m, l = 0.25m, r = 0.2m$	
Dynamics	Total mass = 80kg	$I_z = 39.733kgm^2$
Default	$K_1 = 7, K_{22} = 10, K_{21} = 200$	
Surface	$\mu_1 \in (0.2, 0.4)$	$\mu_2 \in (0.6, 0.8)$

I. presents the parameters used in the entire simulation. In this paper, a sinusoidal waveform is supplied to the wheelchair as the angular orientation, an inclination of 10° and a reference linear velocity of $10m/s$ is also considered. Two surface conditions are analyzed, based on the coefficient of friction of the surface, we refer to these surfaces as; wet surface for $\mu_1 \in (0.2, 0.4)$ and oily surface for $\mu_2 \in (0.6, 0.8)$.

4.1 Wet Surface (μ_1)

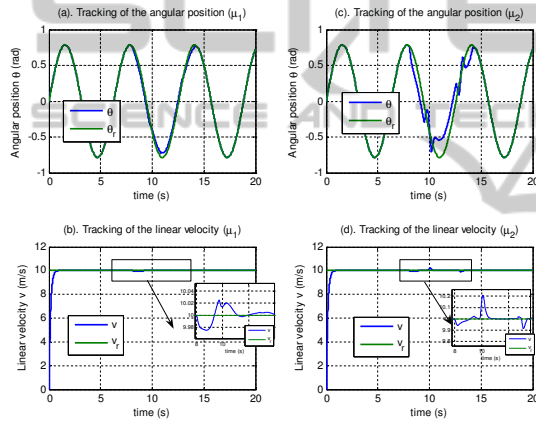


Figure 3: Tracking of orientation and velocity of the platform on wet and oily surfaces.

We use the word wet to mean a condition where only slight slip may occur. A maximum longitudinal coefficient of friction ($\mu_X = 0.2$) and maximum lateral coefficient of friction ($\mu_Y = 0.4$) is therefore considered for a wet surface. In subplot (a) of fig. 3 the reference and the output angular position of the wheelchair is shown. It can be seen that the wheelchair tracked well the reference angular position. The wheelchair then slipped after the 7th second with the introductions of a wet surface, and deviated a little from the reference, however the controller still was able to track the reference orientation during the slip and perfectly after the slip. Subplot (b) of fig. 3 shows the reference and the output linear velocity of the wheelchair. A perfect track of the reference linear velocity is shown throughout the simulation except with a small deviation during the period of slip, this deviation however disappears after slip is eliminated. Torques and errors generated by the wheelchair while moving on wet surface are shown in fig. 4. It may be noticed in subplot

(a) of fig. 4 that the torques supplied to the right and the left wheel increase in magnitude as the wheelchair moves uphill. This is because of the increase in the potential energy of the wheelchair with height.

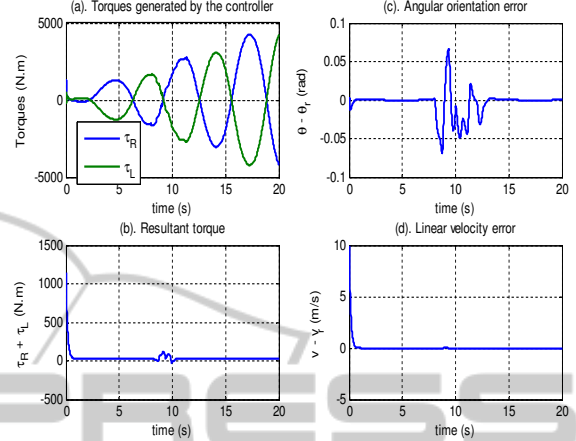


Figure 4: Torques and errors generated by the controller on wet surface.

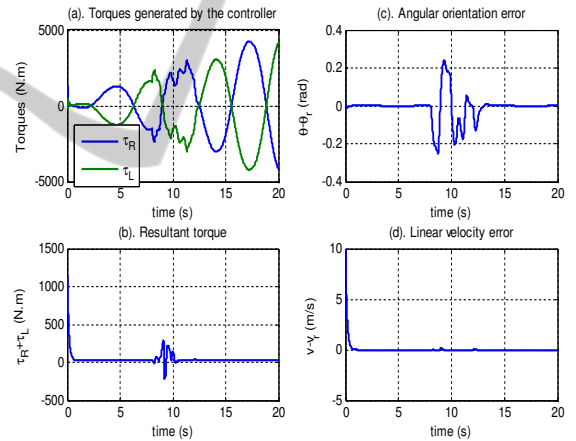


Figure 5: Torques and errors generated by the controller on the oily surface.

4.2 Oily Surface (μ_2)

The word oily is used in this paper to mean a condition with increased slip. A surface with maximum longitudinal coefficient of friction ($\mu_X = 0.8$) and maximum lateral coefficient of friction ($\mu_Y = 0.6$) is considered as oily. Subplot (c) of fig. 3 shows the reference and the output angular position of the wheelchair driven on an oily surface. It can be seen that the wheelchair tracked well the reference angular position however as compared to subplot (a) of the same figure there was an increased deviation during the period of slip indicating that the surface was indeed more slippery. The controller however was

still able to track the reference orientation during the slip and perfectly after the slip verifying the ability of the control law developed. Subplot (d) of fig. 3 shows the reference and the output linear velocity of the wheelchair. A perfect track of the reference linear velocity is again shown throughout the simulation except with a small but increased deviation during the period of slip, this deviation however disappeared after slip was eliminated. Torques and errors generated by the wheelchair while moving on the oily surface are shown in fig. 4.

On both surfaces, during the period of slip, irregular torques were generated to enable the platform track closely the angular orientation and the linear velocity. It may be noticed, however, that highly irregular torques were produced in subplot (a) of fig. 5 than in subplot (a) of fig. 4. This is because of the increased slip on the oily surface. In subplots (c) of fig. 4 and fig. 5, the orientation tracking errors are shown with a deviation of about 0.06 radians and 0.21 radians for wet and oily surfaces respectively. In both cases, the error diminishes with time and the zero error is tracked the just after the 14th second. Little deviations from the reference linear velocity v_r may also noticed in subplots (d) of fig. 4 and fig. 5 during the slip.

4.3 Conclusions

The dynamic model of a wheelchair has been developed in this paper in such a way that the wheelchair movement is not restricted to flat surfaces alone. The model developed here include effects of frictional forces, gravitational forces and slip. Navigation of wheelchair by tracking velocity and orientation is also investigated. A nonlinear feedback law that links the reference linear velocity (v_r) and reference angular orientation (θ_r) supplied to the controller is developed with satisfactory results. Torques supplied to the plant during navigation are also analysed with the result that irregular torques are supplied during slip. Extensive computer simulations are then performed to verify the usefulness of the designed model and controller.

4.4 Future Works

It has been realized that torques supplied to the wheels increases with time as the wheelchair moves uphill, future work may therefore involve limiting the torques supplied to the wheels to a values that may be contained by the supplying battery.

Future work will also involve inclusion of assistive controller to help the wheelchair make realtime

decision in cases where the patient is either unable to or is slow to make such decisions.

Filtering of undesired error signals that might be sent to the controller by severely and shaking disabled wheelchair users and implementation of this controller on the FSATIE wheelchair platform are some of the future works.

ACKNOWLEDGEMENTS

The authors of this paper gratefully appreciate the contribution of Tshwane University of Technology and F'SATIE for providing relevant and necessary support for this research.

REFERENCES

- Dixon, W., Walker, I., and Dawson, D. (2001). Fault detection for wheeled mobile robots with parametric uncertainty. *IEEUASME International Conference on Advanced Intelligent Mechatronics Proceedings*, pages 1245 – 1250.
- Feng, C. and Fei, S. (1998). *Analysis and design of nonlinear control system*. Publishing House of Electronics Industry, Beijing.
- Fierro, R. and Lewis, F. (1997). Control of a nonholonomic mobile robot: Backstepping kinematics into dynamics. *Journal of Robotic Systems*, 14(3):149 – 164.
- Ge, S. and Lewis, F. (2006). *Autonomous mobile robots: sensing, control, decision making and applications*. Taylor and Francis Group LLC,.
- Hamed, E., Yskandar, H., Eric, M., and Imad, M. (2007). Dynamic model of electrical wheelchair with slipping detection. *EUROSIM*, pages 1 – 6.
- Isidori, A. (1995). *Nonlinear Control Systems*. Birkhuser, 3 edition.
- Khalil, H. (1996). *Nonlinear Systems*. Prentice Hall, New Jersey.
- Kozłowski, K. and Pazderski, D. (2004). Modeling and control of a 4-wheel skid steering mobile robot. *International Journal of Applied Mathematics and Computer Science*, 14(4):477 – 496.
- Motte, I. and Guy, C. (2000). A slow manifold approach for the control of mobile robots not satisfying the kinematic constraints. *IEEE Transaction on Robotics and Automation*, 16(6):875 – 880.
- Ortega, R., der Schaft, A. V., Mareels, I., and Maschke, B. (2000). Energy shaping revisited. In *IEEE International Conference on Control Applications*, pages 121–125, Anchorage USA.
- Sidek, S. N. (2008). *Dynamic Modeling and Control of Nonholonomic Wheeled Mobile Robot Subjected To Wheel Slip*. PhD thesis, Graduate School of Vanderbilt University.

- Slotine, J. and Li, W. (1991). *Applied nonlinear control*. Prentice-Hall, Englewood Cliffs, NJ.
- Spong, M. W., Hutchinson, S., and Vidyasagar, M. (1989). *Robot Modeling and Control*. John Wiley & Sons, Inc, 1 edition.
- Stonier, D., Cho, S.-H., Choi, S.-L., Suresh, K. N., and Jong-Hwan, K. (2007). Nonlinear slip dynamics for an omniwheel mobile robot platform. *IEEE International Conference on Robotics and Automation*, pages 2367 – 2372.
- Tarokh, M. and McDermott, G. J. (2005). Kinematics modeling and analyses of articulated rovers. *IEEE Transactions on Robotics*, 21(4):539 – 553.
- Vignier, N., Ravaud, J.-F., Myriam, W., Franois-Xavier, L., and Ville, I. (2008). Demographics of wheelchair users in france: Results of national community based handicaps in capabilities dependence surveys. *Journal of Rehabilitation Medicine*, pages 231 – 239.
- Wells, D. (1967). *Problems of Lagrangian Dynamics Schausms Outline Series*. McGraw Hill Company, New York, 1st edition edition.
- Williams, R. L., Carter, B. E., Paolo, G., and Giulio, R. (2002). Dynamic model with slip for wheeled omnidirectional robots. *IEEE Transaction on Robotics and Automation*, 18(3):285 – 292.
- Wobbrock, J. O., Myers, B. A., Htet, A. H., and LoPresti, E. F. (2004). Text entry from power wheelchairs: Edgewrite for joysticks and touchpads. *ACM*, pages 110 – 117.
- Woude, L. V. D., Groot, S. D., and Janssen, T. (2006). Manual wheelchairs: research and innovation in sports and daily life. *Elsevier*, pages 226 – 235.
- Zhu, X., Dong, G., Hu, D., and Cai, Z. (2006). Robust tracking control of wheeled mobile robots not satisfying nonholonomic constraints. *Proceedings of the Sixth International Conference on Intelligent Systems Design and Applications (ISDA'06)*, page 6.